www.ietdl.org

Published in IET Communications
Received on 25th July 2012
Revised on 6th October 2012
Accepted on 20th November 2012
doi: 10.1049/iet-com.2012.0440

ISSN 1751-8628

Space–time coding scheme for time–frequency asynchronous two-way relay networks

Weile Zhang, Qinye Yin

MOE Key Laboratory for Intelligent Networks and Network Security, Xi'an Jiaotong University, Xi'an 710049, People's Republic of China
E-mail: wlzhang1984@gmail.com

Abstract: In this study, the authors develop a distributed space–time coding scheme for a two-way relay network that contains multiple distributed relay nodes. Both the time and frequency asynchronous nature of the distributed system are considered in the design. Distributed convolutional coding is employed to handle multiple timing errors in the networks. The authors prove that under perfect frequency synchronisation, the proposed scheme can achieve both spatial and multipath diversity by linear receivers, such as linear zero-forcing or minimum mean-square-error receiver, thus providing a low decoding complexity. The authors further find that frequency asynchronism has little effect on the designed scheme and show that the diversity can still be achieved almost surely (in the measured theoretic sense) under both time and frequency asynchronous scenarios. The authors also provide numerical results to corroborate the proposed studies.

1 Introduction

Two-way relay networks (TWRN) have recently attracted much attention [1–3] because of their enhanced spectral efficiency as compared with the conventional one-way relay network (OWRN) [4]. In a typical TWRN consisting of a single user pair and a single relay node, the signals are sent simultaneously from both users to the relay node and are then retransmitted to the two users after necessary processing. After removing the self-interference components, each user can obtain the expected information from the other user. Consequently, the overall communication rate of the two users in TWRN is approximately twice that achieved in OWRN, making TWRN particularly attractive to bidirectional systems [5, 6].

As an efficient way to further improve the bandwidth efficiency of the TWRN, analogue network coding has drawn a lot of interest. Based on the assumption of perfect time and frequency synchronisation, the distributed linear dispersion code and a family of relaying protocols were developed in [7]. However, a cooperative communication system is both time and frequency asynchronous in nature since the multiple transmissions come from distributed users or relay nodes.

Intensive studies on achieving cooperative diversity with time or frequency asynchronism have been made for conventional OWRN [8–13]. However, on the side of TWRN, few works have been reported and most of them considered only time asynchronism. For example, Li *et al.* [14] generalised the Alamouti-like code into an orthogonal frequency-division multiplexing aided TWRN, where cyclic prefix (CP) was exploited to combat timing errors. The unique property of this work was that the fast symbol-wise maximum likelihood (ML) detection can be applied at the destination to achieve diversity. In [15], the distributed convolutional code was exploited to deal with multiple timing errors. The pairwise error probability (PEP) was also computed, from which it demonstrated that both cooperative and multipath diversity can be achieved by the optimal receiver. Another similar work has been proposed in [16], which proved that cooperative diversity can be achieved using only linear receivers, such as linear zero-forcing (ZF), or linear minimum mean-square-error (MMSE) receivers. However, Wang *et al.* [16] assumed a flat fading channel only. Moreover, all these schemes [14–16] assumed perfect frequency synchronisation.

More recently, another space-frequency convolutional coding scheme was designed in [17] for both time and frequency asynchronous amplify-and-forward relay networks, which exploited an extended CP as well as the signal space diversity technique. Although the scheme [17] can be straightforwardly extended to time–frequency asynchronous TWRN, it relies on high-complexity decoding to achieve diversity gain.

In this paper, we propose a distributed space–time coding scheme for TWRN with multiple distributed relay nodes. Both time and frequency asynchronous nature are considered in our design. Convolutional coding is employed to deal with multiple timing errors. The relay nodes implement only simple operations, such as convolution and amplification, and they do not ask for any information about the channels and frequency offsets. The main contributions of this paper are twofold.

First, different from [16], we consider the more general frequency selective fading channels, and we also prove that under perfect frequency synchronisation, the proposed scheme can achieve both spatial and multipath diversity by the linear receivers. It is worth mentioning that [15] adopted the same convolutional coding and proved that diversity can be achieved by the optimal ML receiver. However, in this paper we prove that diversity can be obtained by the linear receivers.

Second, different from both [15, 16] which assumed perfect frequency synchronisation, we consider the frequency offsets among the distributed nodes in the network and find that frequency asynchronism has little effect on our designed scheme. We further show that diversity can still be achieved by the linear receivers almost surely (in the measured theoretical sense) under both time and frequency asynchronous scenarios. Thus, as compared with the existing competitor in [17] which relies on high complexity ML decoding, our proposed scheme can provide a much lower decoding complexity.

The rest of this paper is organised as follows. We present a system model in Section 2. The coding design under frequency synchronous and asynchronous scenarios is developed in Sections 3 and 4, respectively. Simulation results are given in Section 5 and conclusions are drawn in Section 6.

Notations: Superscripts $(\cdot)^*$, $(\cdot)^{\mathrm{T}}$, $(\cdot)^{\mathrm{H}}$, $[\cdot]^{\dagger}$ and $E\{\cdot\}$ represent conjugate, transpose, Hermitian, pseudo inverse and expectation, respectively; $\boldsymbol{j}=\sqrt{-1}$ is the imaginary unit; $\|\boldsymbol{X}\|_F$ denotes the Frobenius norm of $\boldsymbol{X}$, and $\mathrm{diag}\{\cdot\}$ is a diagonal matrix with main diagonal $\{\cdot\}$; $\boldsymbol{I}_N$ denotes the $N\times N$ identity matrix and $\boldsymbol{0}_{M\times N}$ denotes the $M\times N$ matrix with all entries being zero; $\otimes$ denotes linear convolution operation.

2 System model

Consider a TWRN with M relay nodes R_m, $m=1, 2,\ldots,M$, and two terminal nodes T_i, $i=1, 2$, as shown in Fig. 1. Each node is equipped with a single antenna and operates in a half-duplex mode, that is, it cannot simultaneously transmit and receive. Let the two terminals exchange information with the assistance of the relays. Denote

$$\boldsymbol{h}_m=\left[h_m(0), h_m(1), \ldots, h_m(L_h-1)\right]$$
$$\boldsymbol{g}_m=\left[g_m(0), g_m(1), \ldots, g_m(L_g-1)\right]$$

as the channel responses between the relay R_m and two sources T_1, T_2, respectively. We assume $h_m(l)$ and $g_m(l)$ are circularly complex Gaussian random variables with variance $1/L_h$ and $1/L_g$, respectively, such that the channel gains are normalised, that is, $\|\boldsymbol{h}_m\|_F^2=1$ and $\|\boldsymbol{g}_m\|_F^2=1$. The channels are also assumed to be reciprocal in this paper. Nonetheless, the proposed scheme can be straightforwardly extended to more general situations.

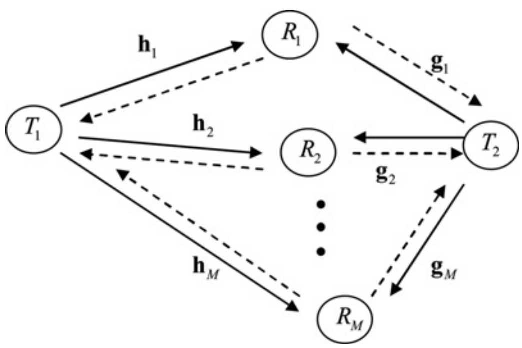

Fig. 1 System model of TWRN, where the solid and dashed lines represent transmission in the first and the second phase, respectively

Suppose terminal T_i, $i=1, 2$, wishes to transmit the N-length signals $\boldsymbol{s}_i=[s_{i,1}, s_{i,2},\ldots,s_{i,N}]$ to the other terminal with average power P_{T}. Denote the delay from T_i to R_m as $\tau_{i,m}^{(1)}$ in the first phase, and define their maximum as $\tau_{i,\max}^{(1)}=\max_{1\le m\le M}\tau_{i,m}^{(1)}$. For notational convenience, we define the following two zero-padded channel vectors

$$\boldsymbol{h}_{\Delta_1,m}=\left[\boldsymbol{0}_{1\times\tau_{1,m}^{(1)}},\quad \boldsymbol{h}_m^{\mathrm{T}},\quad \boldsymbol{0}_{1\times(L_{\max}^{(1)}-L_h-\tau_{1,m}^{(1)})}\right]^{\mathrm{T}}$$
$$\boldsymbol{g}_{\Delta_1,m}=\left[\boldsymbol{0}_{1\times\tau_{2,m}^{(1)}},\quad \boldsymbol{g}_m^{\mathrm{T}},\quad \boldsymbol{0}_{1\times(L_{\max}^{(1)}-L_g-\tau_{2,m}^{(1)})}\right]^{\mathrm{T}}$$

where $L_{\max}^{(1)}=\max\left(L_h+\tau_{1,\max}^{(1)},\quad L_g+\tau_{2,\max}^{(1)}\right)$. By applying the two-way protocol, the signal received at relay node R_m in the first phase can be expressed by a N_1-length vector

$$\boldsymbol{y}_{R_m}=\sqrt{P_T}\boldsymbol{h}_{\Delta_1,m}\otimes\boldsymbol{s}_1+\sqrt{P_T}\boldsymbol{g}_{\Delta_1,m}\otimes\boldsymbol{s}_2+\boldsymbol{n}_{R_m} \tag{1}$$

where $N_1=N+L_{\max}^{(1)}-1$, and $\boldsymbol{n}_{R_m}$ is the corresponding N_1-length additive white Gaussian noise (AWGN) vector with variance $E\left\{\boldsymbol{n}_{R_m}\boldsymbol{n}_{R_m}^{\mathrm{H}}\right\}=\sigma_n^2\boldsymbol{I}_{N_1}$.

In the second phase, the received signal $\boldsymbol{y}_{R_m}$ is linearly convoluted, amplified and then broadcasted to the two terminals simultaneously. For simplicity, we assume that each relay node has equal power constraint P_{R}. After the convolution and amplifying process, the transmitted signal at R_m becomes

$$\boldsymbol{x}_{R_m}=\alpha\cdot\boldsymbol{t}_m\otimes\boldsymbol{y}_{R_m} \tag{2}$$

where $\boldsymbol{t}_m=[t_{m,0},\quad t_{m,1},\ldots,t_{m,Q-1}]^{\mathrm{T}}$ denotes the normalised Q-length generator vector to be designed later. The vector is normalised such that $\|\boldsymbol{t}_m\|_F^2=1$. Meanwhile, the amplification factor is taken as

$$\alpha=\sqrt{\frac{P_{\mathrm{R}}N_1}{2NP_{\mathrm{T}}+N_1\sigma_n^2}}$$

to meet the average power constraint. A brief proof can be found in Appendix 1.

Owing to the symmetry, we explain only the process at T_1. Denote the delay from R_m to T_i as $\tau_{i,m}^{(2)}$, and define $\tau_{i,\max}^{(2)}=\max_{1\le m\le M}\tau_{i,m}^{(2)}$. Then, the received signal at terminal T_1 can be expressed by an N_2-length vector

$$\begin{aligned}\boldsymbol{z}_{T_1}&=\sum_{m=1}^{M}\boldsymbol{h}_{\Delta_2,m}\otimes\boldsymbol{x}_{R_m}+\boldsymbol{n}_{T_1}\\&=\sum_{m=1}^{M}\alpha\boldsymbol{h}_{\Delta_2,m}\otimes\boldsymbol{t}_m\otimes\boldsymbol{y}_{R_m}+\boldsymbol{n}_{T_1}\end{aligned} \tag{3}$$

IET Commun., 2013, Vol. 7, Iss. 2, pp. 137–145
doi: 10.1049/iet-com.2012.0440

where

$$\boldsymbol{h}_{\Delta_2,m} = \left[\boldsymbol{0}_{1\times\tau_{1,m}^{(2)}}, \quad \boldsymbol{h}_m^{\mathrm{T}}, \quad \boldsymbol{0}_{1\times\left(\tau_{1,\boldsymbol{m}}^{(2)}-\tau_{1,m}^{(2)}\right)}\right]^{\mathrm{T}}$$

$$N_2 = N_1 + L_h + \tau_{1,\max}^{(2)} + Q - 2$$

and $\boldsymbol{n}_{T_1}$ is the corresponding N_2-length AWGN vector with variance $E\left\{\boldsymbol{n}_{T_1}\boldsymbol{n}_{T_1}^{\mathrm{H}}\right\} = \sigma_n^2 I_{N_2}$.

Substituting (1) into (3), and cancelling backward self-interference signal related to $\boldsymbol{s}_1$, we obtain

$$\begin{aligned}\boldsymbol{y}_{T_1} &= \sum_{m=1}^{M} \alpha\sqrt{P_{\mathrm{T}}}\boldsymbol{h}_{\Delta_2,m} \otimes \boldsymbol{t}_m \otimes \boldsymbol{g}_{\Delta_1,m} \otimes \boldsymbol{s}_2 + \boldsymbol{w}_{T_1} \\ &= \alpha\sqrt{P_{\mathrm{T}}}\boldsymbol{H}\boldsymbol{s}_2 + \boldsymbol{w}_{T_1} \end{aligned} \tag{4}$$

where

$$\boldsymbol{H} = \mathcal{T}^{(N)}[\boldsymbol{h}_e], \quad \boldsymbol{h}_e = \sum_{m=1}^{M} \boldsymbol{h}_{\Delta_2,m} \otimes \boldsymbol{t}_m \otimes g_{\Delta_1,m}$$

$$\boldsymbol{w}_{T_1} = \mathbf{n}_{T_1} + \sum_{m=1}^{M} \alpha\boldsymbol{h}_{\Delta_2,m} \otimes \boldsymbol{t}_m \otimes \boldsymbol{n}_{R_m}$$

and $\mathcal{T}^{(K)}[\boldsymbol{x}]$ is a Toeplitz matrix in the following form

$$\mathcal{T}^{(K)}[\boldsymbol{x}] = \underbrace{\begin{bmatrix} x_1 & \cdots & 0 \\ \vdots & \ddots & \vdots \\ x_P & \ddots & x_1 \\ \vdots & \ddots & \vdots \\ 0 & \cdots & x_P \end{bmatrix}}_{K \text{ columns}}$$

for any vector $\boldsymbol{x} = [x_1, x_2, \ldots, x_P]^{\mathrm{T}}$.

3 Distributed convolutional coding with linear receiver

By defining

$$\boldsymbol{v}_m = \boldsymbol{h}_m \otimes \boldsymbol{g}_m, \quad L = L_g + L_h - 1$$

$$\boldsymbol{t}_{\Delta,m} = \left[\boldsymbol{0}_{1\times\left(\tau_{2,m}^{(1)}+\tau_{1,m}^{(2)}\right)}, \quad \boldsymbol{t}_m^{\mathrm{T}}, \quad 0_{1\times(L_{\max}^{(1)}-L_g-\tau_{2,m}^{(1)}+\tau_{1,\max}^{(2)}-\tau_{1,m}^{(2)})}\right]^{\mathrm{T}}$$

we rewrite $\boldsymbol{h}_e$ as

$$\boldsymbol{h}_e = \sum_{m=1}^{M} \boldsymbol{t}_{\Delta,m} \otimes \boldsymbol{v}_m = \sum_{m=1}^{M} \mathcal{T}^{(L)}[\boldsymbol{t}_{\Delta,m}]\boldsymbol{v}_m = \Theta_\Delta \boldsymbol{v} \tag{5}$$

where

$$\Theta_\Delta = \left[\mathcal{T}^{(L)}[\boldsymbol{t}_{\Delta,1}], \quad \mathcal{T}^{(L)}[\boldsymbol{t}_{\Delta,2}], \quad \ldots, \quad \mathcal{T}^{(L)}[\boldsymbol{t}_{\Delta,M}]\right]$$

$$\boldsymbol{v} = \left[\boldsymbol{v}_1^{\mathrm{T}}, \boldsymbol{v}_2^{\mathrm{T}}, \ldots, \boldsymbol{v}_M^{\mathrm{T}}\right]^{\mathrm{T}}$$

The following lemma provides the condition that can guarantee achievement of cooperative and multipath diversity with a linear ZF or an MMSE receiver:

Lemma 1: For PAM, PSK and square QAM, if $\boldsymbol{\Theta}_{\boldsymbol{\Delta}}$ has a full column rank under any delay profile, then the proposed scheme can achieve both cooperative and multipath diversity $M \cdot \min\{L_g, L_h\}$ with a linear ZF or an MMSE receiver.

Proof: See Appendix 2.

Lemma 1 tells us that we need to carefully design the convolutional vectors $\boldsymbol{t}_m$ such that the matrix $\boldsymbol{\Theta}_{\boldsymbol{\Delta}}$ always has full column rank under any delay profile. This is related to the shift-full-rank (SFR) matrices [10, 11]. Note that, in previous works [11], the construction criteria of SFR matrices under multipath fading have been studied. Thus, we directly adopt the designs in [11]. We provide some design examples in Table 1.

Remark: Note that [15] considered the optimal ML receiver and arrived at the same diversity order $M \cdot \min\{L_g, L_h\}$ via PEP analysis. However, we prove that diversity can be achieved by the linear receivers, which is one of the contributions in this work.

4 Frequency asynchronous cooperation

We denote the oscillator frequencies of the two terminals and relays by f_{T_i}, $i = 1, 2$ and f_{R_m}, $m = 1, 2, \ldots, M$, respectively. Then, in the first phase, the received signal at the relay node R_m becomes

$$\begin{aligned}\underline{\boldsymbol{y}}_{R_m} &= \sqrt{P_{\mathrm{T}}}\boldsymbol{\Phi}^{(N_1)}\left[f_{T_1} - f_{R_m}\right]\left(\boldsymbol{h}_{\Delta_1,m} \otimes \boldsymbol{s}_1\right) \\ &\quad + \sqrt{P_{\mathrm{T}}}\boldsymbol{\Phi}^{(N_1)}\left[f_{T_2} - f_{R_m}\right]\left(\boldsymbol{g}_{\Delta_1,m} \otimes \boldsymbol{s}_2\right) + \boldsymbol{n}_{R_m}\end{aligned} \tag{6}$$

where

$$\boldsymbol{\Phi}^{(K)}[f] = \mathrm{diag}\left\{1, \mathrm{e}^{\mathrm{j}2\pi f T_s}, \ldots, \mathrm{e}^{\mathrm{j}2\pi(K-1)fT_s}\right\}$$

Table 1 Convolutional vector examples

	$\boldsymbol{t}_m^{\mathrm{T}}$
$M = 2$, $L = 1$	$\frac{1}{\sqrt{2}}[1, 1]$, $\frac{1}{\sqrt{2}}[1, -1]$
$M = 3$, $L = 1$	$\frac{1}{\sqrt{3}}[1, 1, 1]$, $\frac{1}{\sqrt{6}}[1, -2, 1]$, $\frac{1}{\sqrt{2}}[1, 0, -1]$
$M = 2$, $L = 3$	$\frac{1}{\sqrt{2}}[1, 0, 0, 1]$, $\frac{1}{\sqrt{2}}[1, 0, 0, -1]$
$M = 3$, $L = 3$	$\frac{1}{\sqrt{3}}[1, 0, 0, 1, 0, 0, 1]$, $\frac{1}{\sqrt{6}}[1, 0, 0, -2, 0, 0, 1]$, $\frac{1}{\sqrt{2}}[1, 0, 0, 0, 0, 0, -1]$

denotes the diagonal matrix reflecting the phase rotation introduced by frequency offsets, with T_s being the sampling period.

In the second phase, each relay node conducts convolution and amplification for the received signal $\underline{\boldsymbol{y}}_{R_m}$ and then broadcasts. Terminal T_1 receives

$$\underline{\boldsymbol{z}}_{T_1} = \alpha\sum_{m=1}^{M}\phi_m\boldsymbol{\Phi}^{(N_2)}\left[f_{R_m} - f_{T_1}\right]\left(\boldsymbol{h}_{\Delta_2,m}\otimes\boldsymbol{t}_m\otimes\underline{\boldsymbol{y}}_{R_m}\right) + \boldsymbol{n}_{T_1} \quad (7)$$

where $\phi_m = \mathrm{e}^{\mathrm{j}2\pi N_1(f_{R_m}-f_{T_1})T_s}$ stands for cumulative phase rotation in the first phase. Substituting (6) into (7) and cancelling the self-interference, terminal T_1 obtains

$$\begin{aligned}\underline{\boldsymbol{y}}_{T_1} &= \alpha\sqrt{P_T}\sum_{m=1}^{M}\phi_m\boldsymbol{\Phi}^{(N_2)}\left[f_{R_m} - f_{T_1}\right]\\ &\quad\times\left(\boldsymbol{h}_{\Delta_2,m}\otimes\boldsymbol{t}_m\otimes\left(\boldsymbol{\Phi}^{(N_1)}\left[f_{T_2} - f_{R_m}\right]\left(\boldsymbol{g}_{\Delta_1,m}\otimes\boldsymbol{s}_2\right)\right)\right)\\ &\quad + \underline{\boldsymbol{w}}_{T_1}\end{aligned} \quad (8)$$

where

$$\begin{aligned}\underline{\boldsymbol{w}}_{T_1} &= \boldsymbol{n}_{T_1} + \alpha\sum_{m=1}^{M}\phi_m\Phi^{(N_2)}\left[f_{R_m} - f_{T_1}\right]\\ &\quad\times\left(\boldsymbol{h}_{\Delta_2,m}\otimes\boldsymbol{t}_m\otimes\mathbf{n}_{R_m}\right)\end{aligned} \quad (9)$$

Note that

$$\begin{aligned}&\boldsymbol{h}_{\Delta_2,m}\otimes\boldsymbol{t}_m\otimes\left(\Phi^{(N_1)}[f_{T_2} - f_{R_m}]\left(\boldsymbol{g}_{\Delta_1,m}\otimes\boldsymbol{s}_2\right)\right)\\ &\quad = \mathcal{T}^{(N_1)}[\boldsymbol{h}_{\Delta_2,m}\otimes\underline{\boldsymbol{t}}_m]\Phi^{(N_1)}[f_{T_2} - f_{R_m}]\left(\boldsymbol{g}_{\Delta_1,m}\otimes\boldsymbol{s}_2\right)\end{aligned} \quad (10)$$

Then, according to Lemma 1 in [18], we obtain

$$\begin{aligned}&\mathcal{T}^{(N_1)}\left[\boldsymbol{h}_{\Delta_2,m}\otimes\underline{\boldsymbol{t}}_m\right]\boldsymbol{\Phi}^{(N_1)}\left[f_{T_2} - f_{R_m}\right]\\ &\quad = \boldsymbol{\Phi}^{(N_2)}\left[f_{T_2} - f_{R_m}\right]\mathcal{T}^{(N_1)}\left[\boldsymbol{\Phi}^{(N_3)}\left[f_{R_m} - f_{T_2}\right]\left(\boldsymbol{h}_{\Delta_2,m}\otimes\boldsymbol{t}_m\right)\right]\end{aligned} \quad (11)$$

where $N_3 = L_h + \tau^{(2)}_{1,\max} + Q - 1$ is the length of $\boldsymbol{h}_{\Delta_2,m}\otimes\boldsymbol{t}_m$. By substituting (10) and (11) into (8), we rewrite $\underline{\boldsymbol{y}}_{T_1}$ as follows

$$\begin{aligned}\underline{\boldsymbol{y}}_{T_1} &= \alpha\sqrt{P_T}\boldsymbol{\Phi}^{(N_2)}\left[f_{T_2} - f_{T_1}\right]\\ &\quad\times\sum_{m=1}^{M}\phi_m\left(\mathcal{T}^{(N_1)}\left[\boldsymbol{\Phi}^{(N_3)}\left[f_{R_m} - f_{T_2}\right]\left(\boldsymbol{h}_{\Delta_2,m}\otimes\boldsymbol{t}_m\right)\right]\right.\\ &\quad\left.\times\left(\boldsymbol{g}_{\Delta_1,m}\otimes\boldsymbol{s}_2\right)\right) + \underline{\boldsymbol{w}}_{T_1}\end{aligned} \quad (12)$$

We then derive

$$\begin{aligned}&\boldsymbol{\Phi}^{(N_3)}\left[f_{R_m} - f_{T_2}\right]\left(\boldsymbol{h}_{\Delta_2,m}\otimes\mathbf{t}_m\right)\\ &\quad = \boldsymbol{\Phi}^{(N_3)}\left[f_{R_m} - f_{T_2}\right]\mathcal{T}^{\left(L_h + \tau^{(2)}_{1,\max}\right)}[\boldsymbol{t}_m]h_{\Delta_2,m}\end{aligned} \quad (13)$$

Again, using the converse transition of Lemma 1 in [18], there is

$$\begin{aligned}&\boldsymbol{\Phi}^{(N_3)}\left[f_{R_m} - f_{T_2}\right]\mathcal{T}^{\left(L_h + \tau^{(2)}_{1,\max}\right)}[\boldsymbol{t}_m]\\ &\quad = \mathcal{T}^{\left(L_h + \tau^{(2)}_{1,\max}\right)}\left[\Phi^{(Q)}\left[f_{R_m} - f_{T_2}\right]\boldsymbol{z}\boldsymbol{t}_m\right]\boldsymbol{\Phi}^{\left(L_h + \tau^{(2)}_{1,\max}\right)}\\ &\qquad\left[f_{R_m} - f_{T_2}\right]\end{aligned} \quad (14)$$

Substituting (14) into (13) yields

$$\begin{aligned}&\boldsymbol{\Phi}^{(N_3)}\left[f_{R_m} - f_{T_2}\right]\left(\boldsymbol{h}_{\Delta_2,m}\otimes\boldsymbol{t}_m\right)\\ &\quad = \left(\boldsymbol{\Phi}^{(Q)}\left[f_{R_m} - f_{T_2}\right]\boldsymbol{t}_m\right)\\ &\qquad\otimes\left(\boldsymbol{\Phi}^{\left(L_h + \tau^{(2)}_{1,\max}\right)}[f_{R_m} - f_{T_2}]h_{\Delta_2,m}\right)\end{aligned} \quad (15)$$

By defining

$$\underline{\boldsymbol{h}}_{\Delta_2,m} = \phi_m\boldsymbol{\Phi}^{\left(L_h + \tau^{(2)}_{1,\max}\right)}\left[f_{R_m} - f_{T_2}\right]\boldsymbol{h}_{\Delta_2,m}$$

Equation (12) can be simplified to

$$\begin{aligned}\underline{\boldsymbol{y}}_{T_1} &= \alpha\sqrt{P_T}\boldsymbol{\Phi}^{(N_2)}\left[f_{T_2} - f_{T_1}\right]\\ &\quad\times\sum_{m=1}^{M}\left(\left(\boldsymbol{\Phi}^{(Q)}\left[f_{R_m} - f_{T_2}\right]\boldsymbol{t}_m\right)\otimes\underline{\boldsymbol{h}}_{\Delta_2,m}\otimes\boldsymbol{g}_{\Delta_1,m}\otimes\boldsymbol{s}_2\right)\\ &\quad + \underline{\boldsymbol{w}}_{T_1}\end{aligned} \quad (16)$$

Similarly, we define

$$\underline{\boldsymbol{h}}_e = \sum_{m=1}^{M}\left(\left(\boldsymbol{\Phi}^{(Q)}[f_{R_m} - f_{T_2}]\boldsymbol{t}_m\right)\otimes\underline{\boldsymbol{h}}_{\Delta_2,m}\otimes\boldsymbol{g}_{\Delta_1,m}\right)$$

$$\underline{\boldsymbol{H}} = \mathcal{T}^{(N)}[\underline{\boldsymbol{h}}_e]$$

and then (16) can be rewritten as

$$\underline{\boldsymbol{y}}_{T_1} = \alpha\sqrt{P_T}\boldsymbol{\Phi}^{(N_2)}\left[f_{T_2} - f_{T_1}\right]\cdot\underline{\boldsymbol{H}}\boldsymbol{s}_2 + \underline{\boldsymbol{w}}_{T_1} \quad (17)$$

which arrives at a similar format as (4). An important observation is made here that the received signal model of (17) is equivalent to the situation that signal $\boldsymbol{s}_2$ transmitted by T_2 directly arrives at T_1 after experiencing channel response $\underline{\boldsymbol{h}}_e$. There appears only one frequency offset $f_{T2} - f_{T1}$ left at terminal T_1, which can be easily compensated.

By denoting

$$\underline{\boldsymbol{v}}_m = \phi_m\mathrm{e}^{\mathrm{j}2\pi\tau^{(2)}_{1,m}\left(f_{R_m} - f_{T_2}\right)T_s}\left(\Phi^{(L_h)}\left[f_{R_m} - f_{T_2}\right]\boldsymbol{h}_m\right)\otimes\boldsymbol{g}_m$$

$$\begin{aligned}\underline{\boldsymbol{t}}_{\Delta,m} = &\left[\mathbf{0}_{1\times\left(\tau^{(1)}_{2,m} + \tau^{(2)}_{1,m}\right)},\quad \boldsymbol{t}_m^{\mathrm{T}}\Phi^{(Q)}\left[f_{R_m} - f_{T_2}\right],\right.\\ &\left.\times\,\mathbf{0}_{1\times\left(L^{(1)}_{\max} - L_g - \tau^{(1)}_{2,m} + \tau^{(2)}_{1,\max} - \tau^{(2)}_{1,m}\right)}\right]^{\mathrm{T}}\end{aligned}$$

we obtain

$$\underline{\boldsymbol{h}}_e = \underline{\boldsymbol{\Theta}}_{\boldsymbol{\Delta}}\underline{\boldsymbol{v}} \quad (18)$$

IET Commun., 2013, Vol. 7, Iss. 2, pp. 137–145
doi: 10.1049/iet-com.2012.0440

where

$$\underline{\boldsymbol{\Theta}}_{\Delta} = \left[\mathcal{T}^{(L)}[\underline{\boldsymbol{t}}_{\Delta,1}], \mathcal{T}^{(L)}[\underline{\boldsymbol{t}}_{\Delta,2}], \ldots, \mathcal{T}^{(L)}[\underline{\boldsymbol{t}}_{\Delta,M}]\right]$$
$$\underline{\boldsymbol{v}} = \left[\underline{\boldsymbol{v}}_1^{\mathrm{T}}, \underline{\boldsymbol{v}}_2^{\mathrm{T}}, \ldots, \underline{\boldsymbol{v}}_M^{\mathrm{T}}\right]^{\mathrm{T}}$$

Since $\underline{\boldsymbol{v}}_m$ has the same statistical behaviour with $\boldsymbol{v}_m$, we can directly apply Lemma 1 and draw the conclusion that a diversity of $M \cdot \min\{L_g, L_h\}$ can be achieved with linear receivers, when $\underline{\boldsymbol{\Theta}}_{\boldsymbol{\Delta}}$ has full-column rank under any delay profile, that is, $\underline{\boldsymbol{\Theta}}_{\boldsymbol{\Delta}}$ is an SFR matrix. Different from $\boldsymbol{\Theta}_{\Delta}$, each submatrix of $\underline{\boldsymbol{\Theta}}_{\boldsymbol{\Delta}}$, that is, $\mathcal{T}^{(L)}[\underline{\boldsymbol{t}}_{\Delta,m}]$ is affected by the frequency offset between relay R_m and T_2 individually. Since the relay nodes are assumed to have no knowledge of any frequency offset information between themselves and the terminals, we provide the following lemma:

Lemma 2: If the convolutional vector $\boldsymbol{t}_m$ is designed such that $\boldsymbol{\Theta}_{\boldsymbol{\Delta}}$ always has a full column rank under any delay profile, then the matrix $\underline{\boldsymbol{\Theta}}_{\boldsymbol{\Delta}}$ will almost surely (in the measured theoretical sense) have full column rank under frequency asynchronism with any delay profile. □

Proof: See Appendix 3.

Lemma 2 tells us that, with frequency asynchronism, we can still adopt the convolutional vectors that are originally designed for the frequency synchronous scenarios. The multiple frequency offsets will not affect diversity almost surely (in the measured theoretical sense).

5 Simulations

In this section, we provide simulation results to examine our studies. Each block contains $N = 32$ BPSK data symbols. Unless otherwise stated, we let the terminal nodes adopt ZF decoding, and assume that they have perfect knowledge of the channels and frequency offsets. The convolutional vectors are selected from Table 1 according to the number of relay nodes and the value of L. Moreover, the performance under both flat fading channel and frequency selective fading channel with two paths, that is, $L_g = 2$ and $L_h = 2$, are considered, which are referred to as 'flat' and 'fre', respectively. For each round of simulation, the random delays $\tau_{i,m}^{(1)}$ and $\tau_{i,m}^{(2)}$, $m = 1, 2, \ldots, M$, $i = 1, 2$, are uniformly selected from the set $\{0, 1, 2, 3\}$. The entries of the channel vectors $\boldsymbol{h}_m$ and $\boldsymbol{g}_m$ follow complex Gaussian distribution with variance $1/L_h$ and $1/L_g$, respectively.

First, we consider that perfect frequency synchronisation is achieved in the network. We denote P as the total average power of the whole network and let a portion of $\beta \cdot P$ be allocated to the two terminals and the rest $(1 - \beta) \cdot P$ is assigned to M relays, that is, $P_T = \beta \cdot P/2$ and $P_R = (1 - \beta) \cdot P/M$. In Fig. 2, we investigate the bit-error rate (BER) performance under different power allocation schemes by changing β from 0.1 to 0.9. We fix P/σ_n^2 as 35 dB in this example and consider both two-relay and three-relay scenarios. The four curves in this figure suggest that there is an optional range of β that can be selected without considerable loss of performance among these scenarios, for example, from 0.3 to 0.5 in this example. Without loss of generality, we choose $\beta = 0.5$ in our following evaluations, and define P_T/σ_n^2 as the system signal-to-noise ratio (SNR).

Fig. 3 depicts the BER performance as a function of SNR for $M = 2$ and $M = 3$ relay nodes. To demonstrate the achieved diversity of our scheme, we also include the performance of standard 2×1 and 2×2 co-located multiple-in multiple-out (MIMO) systems with Alamouti coding, whose diversity order are two and four, respectively. It is seen apparently that our relay scheme performs much worse than the standard MIMO systems. This is because the signal transmission in our scheme experiences two fading processes, that is, from one terminal to the relay nodes and then from the relay nodes to the other terminal. In addition, our relay scheme also suffers from noise propagation from the relay nodes to the terminal nodes. However, we see that in the high SNR region, the curves of our scheme corresponding to two relays under flat fading channels are nearly parallel with the curve of 2×1 MIMO. We can also observe the diversity improvement of our scheme under frequency selective channels. These verify that our scheme can achieve both spatial and multipath diversity, which coincides with our analysis.

Next, we consider the frequency asynchronous scenarios. The normalised frequency offsets between R_m and T_2 and between T_1 and T_2 are defined as $\xi_m = (f_{R_m} - f_{T_2})NT_s$ and $\xi_T = (f_{T_1} - f_{T_2})NT_s$, respectively. For each round of

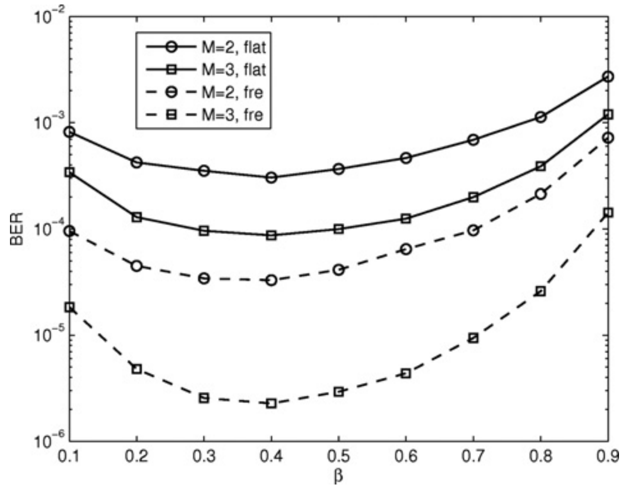

Fig. 2 BER performance of our scheme with different power allocation schemes under both flat and frequency selective channels

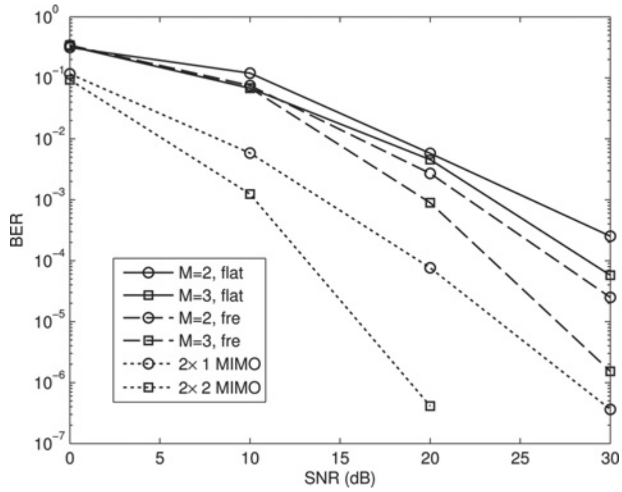

Fig. 3 BER performance of our scheme against SNR under both flat and frequency selective fading channels with perfect frequency synchronisation

doi: 10.1049/iet-com.2012.0440

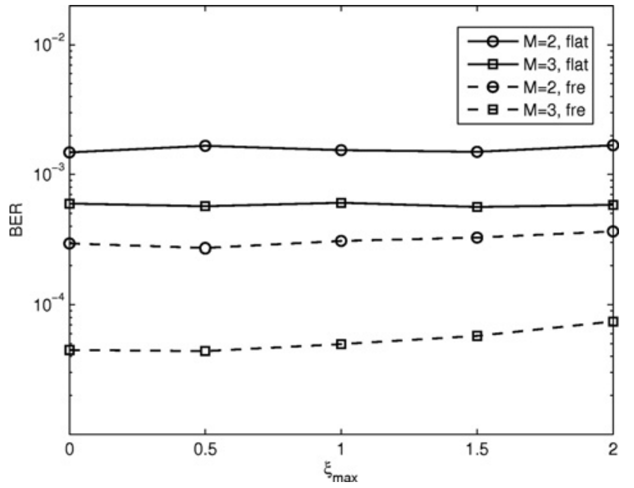

Fig. 4 BER performance of our scheme against $\xi_{\max}$ under both flat and frequency selective fading channels (SNR = 25 dB)

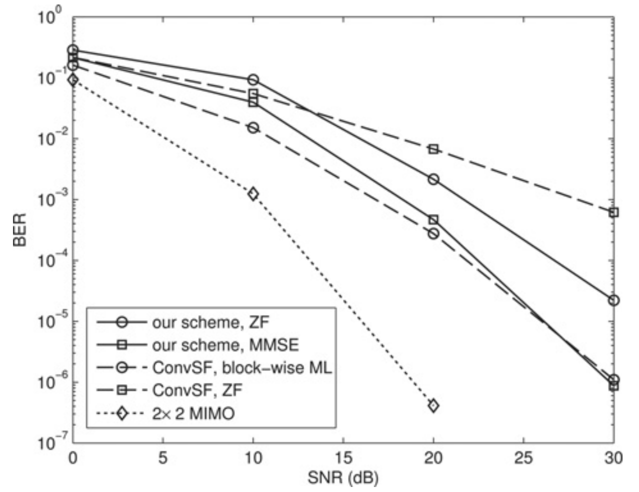

Fig. 6 *BER performance comparison between our scheme and ConvSF [17] under frequency asynchronous scenarios*

simulation, we assume ξ_m and ξ_T are randomly generated from $-\xi_{\max}$ to $\xi_{\max}$. The BER performance of our scheme against $\xi_{\max}$ under different scenarios is shown in Fig. 4, where the SNR is set as 25 dB. The results clearly demonstrate that under both flat and frequency selective fading channels, the existence of frequency asynchronism has little effect on the BER performance of our scheme.

Then, we show the BER performance comparison against SNR of our scheme between frequency synchronous and asynchronous scenarios in Fig. 5, represented by the solid and dashed curves, respectively. We set $\xi_{\max} = 1$ in the frequency asynchronous scenarios. Clearly, for both the two-relay and three-relay cases, the curves with frequency asynchronism almost overlap with the corresponding ones under perfect frequency synchronisation. This once again verifies that our scheme works well and can achieve both spatial and multipath diversity under the frequency asynchronous scenarios.

In Fig. 6, we compare the BER performance of our scheme under frequency asynchronous scenarios between ZF and MMSE decoding. The performance of the space frequency convolutional coding scheme proposed in [17] is also included, referred to as 'ConvSF'. In this example, we consider two relays and frequency selective channels, and assume $\xi_{\max} = 1$. The encoding size is set as four in ConvSF. As expected, MMSE decoding can significantly improve the BER performance of our scheme. It is also seen that, with block-wise ML decoding, ConvSF also works well in both the time and frequency asynchronous scenarios. It not only nearly achieves spatial and multipath diversity, but also obtains similar performance to our scheme with MMSE decoding. However, as we have mentioned earlier, ConvSF suffers from a substantial loss of both BER performance and diversity when low-complexity ZF decoding is adopted.

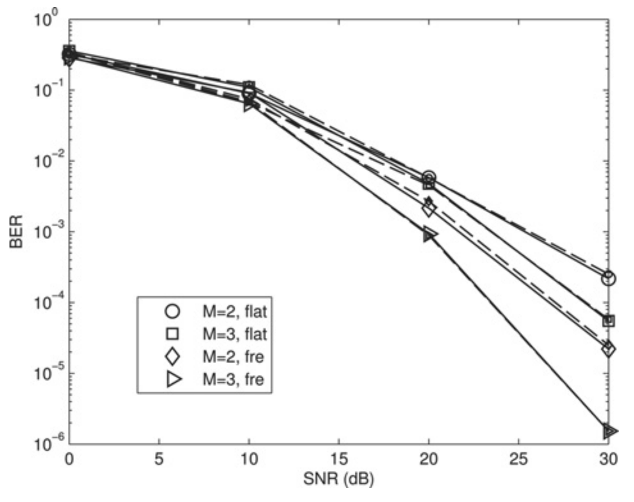

Fig. 5 BER comparison of our scheme between frequency synchronous and asynchronous scenarios, represented by the solid and dashed curves, respectively

6 Conclusions

In this paper, we proposed a distributed space–time coding scheme for time–frequency asynchronous TWRN. It was proved that, under time asynchronism or time–frequency asynchronism, the proposed scheme could achieve both cooperative and multipath diversity with linear receivers. Numerical results were provided to verify our studies.

7 Acknowledgment

This paper was presented in part at the IEEE Global Telecommunication Conference (GLOBECOM), Houston, USA, on December 2011. This work was supported by the National Science and Technology Major Project of China under Grant No. 2010ZX03003-002-02, the National Natural Science Foundation of China under Grants No. 60971113, 61071125, 61071216, 61172093, 61172092 and 61102081, and the Science Foundation for Innovative Research Group of China under Grant No. 60921003.

8 References

1 Zhang, S., Liew, S.C., Lam, P.P.: 'Physical-layer network coding'. Proc. MobiCom, Los Angeles, USA, September 2006, pp. 358–365
2 Li, C., Yang, L., Zhu, W.P.: 'Minimum mean squared error design of single-antenna two-way distributed relays based on full or partial channel state information', *IET Commun.*, 2011, **5**, (5), pp. 728–735
3 Yang, Y., Ge, J.H., Ji, Y.C., Gao, Y.: 'Performance analysis and instantaneous power allocation for two-way opportunistic amplify-and forward relaying', *IET Commun.*, 2011, **5**, (10), pp. 1430–1439

4 Laneman, J.N., Tse, D.N.C., Wornell, G.W.: 'Cooperative diversity in wireless networks: efficient protocols and outage behavior', *IEEE Trans. Inf. Theory*, 2004, **50**, (12), pp. 3062–3080
5 Rankov, B., Wittenben, A.: 'Spectral efficient protocols for halfduplex fading relay channels', *IEEE J. Sel. Areas Commun.*, 2007, **25**, (2), pp. 379–389
6 Akino, T.K., Popovski, P., Tarokh, V.: 'Optimized constellation for two-way wireless relaying with physical network coding', *IEEE J. Sel. Areas Commun.*, 2009, **27**, (5), pp. 773–787
7 Cui, T., Gao, F., Nallanathan, A.: 'Distributed space-time coding for two-way wireless relay networks'. Proc. IEEE ICC, Dresden, Germany, June 2009, pp. 511–516
8 Mei, Y., Hua, Y., Swami, A., *et al*: 'Combating synchronization errors in cooperative relays'. Proc. IEEE ICASSP, Philadelphia, USA, 2005, pp. 369–372
9 Shang, Y., Xia, X.G.: 'Shift full rank matrices and applications in space-time trellis codes for relay networks with asynchronous cooperative diversity', *IEEE Trans. Inf. Theory*, 2006, **52**, (7), pp. 3153–3167
10 Guo, X., Xia, X.G.: 'Distributed linear convolutive space-time codes for asynchronous cooperative communication networks', *IEEE Trans. Wirel. Commun.*, 2008, **7**, (5), pp. 1857–1861
11 Zhang, Z., Zhu, S., Nallanathan, A.: 'Distributed space-time trellis code for asynchronous cooperative communications under frequency-selective channels', *IEEE Trans. Wirel. Commun.*, 2009, **8**, (2), pp. 796–805
12 Li, Z., Xia, X.G.: 'An Alamouti coded OFDM transmission for cooperative systems robust to both timing errors and frequency offsets', *IEEE Trans. Wirel. Commun.*, 2008, **7**, (2), pp. 1839–1844
13 Zhang, W., Wang, H., Yin, Q., *et al*: 'Space frequency code for cooperative communications with both timing errors and carrier frequency offsets', *IEICE Trans. Commun.*, 2010, **E93-B**, (12), pp. 3505–3508
14 Li, Z., Xia, X.G., Li, B.: 'Achieving full diversity and fast ML decoding via simple analog network coding for asynchronous two-way relay networks', *IEEE Trans. Commun.*, 2009, **57**, (12), pp. 3672–3681
15 Zhong, Z., Zhu, S., Lv, G.: 'Distributed space-time code for asynchronous two-way wireless relay networks under frequency-selective channels'. Proc. ICC, Dresden, Germany, June 2009, pp. 1–5
16 Wang, H., Xia, X.G., Yin, Q.: 'A linear analog network coding for asynchronous two-way relay networks', *IEEE Trans. Wirel. Commun.*, 2010, **9**, (12), pp. 3630–3637
17 Zhang, W.L., Gao, F.F., Yin, Q.Y., Wang, H.M.: 'Space-frequency convolutional coding for frequency-asynchronous AF relay networks', *IEEE Trans. Veh. Technol.*, 2012, **61**, (5), pp. 2412–2417
18 Wang, G., Gao, F., Wu, Y.C., *et al*: 'Joint CFO and channel estimation for ZP-OFDM modulated two-way relay networks'. Proc. WCNC, Sydney, April 2010, pp. 1–6
19 Liu, J., Zhang, J.K., Wong, K.M.: 'Full-diversity codes for MISO systems equipped with linear or ML detectors', *IEEE Trans. Inf. Theory*, 2008, **54**, (10), pp. 4511–4527
20 Jing, Y., Hassibi, B.: 'Distributed space-time coding in wireless relay networks', *IEEE Trans. Wirel. Commun.*, 2006, **5**, (12), pp. 3524–3536
21 Zhang, W., Li, Y., Xia, X.G., *et al*: 'Distributed space-frequency coding for cooperative diversity in broadband wireless Ad Hoc networks', *IEEE Trans. Wirel. Commun.*, 2008, **7**, (3), pp. 995–1003
22 Jiang, T., Sidiropoulos, N.D., Berge, J.M.F.: 'Almost-sure identifiability of multidimensional harmonic retrieval', *IEEE Trans. Signal Process.*, 2001, **49**, (9), pp. 1849–1859

9 Appendix 1

9.1 Amplification factor

The power of the received signal $\boldsymbol{y}_{R_m}$ at the first phase can be expressed as $2NP_T + N_1\sigma_n^2$. Since the convolutional vector $\boldsymbol{t}_m$ is normalised, the power of the signal transmitted by each relay node is given by $\alpha^2(2NP_T + N_1\sigma_n^2) = P_R N_1$. Thereby, we obtain

$$\alpha = \sqrt{\frac{P_R N_1}{2NP_T + N_1\sigma_n^2}}$$

10 Appendix 2

10.1 Proof of Lemma 1

Before our proof, we cite the results from [19] in the following properties.

Property 1: ([19]) If $\boldsymbol{H}^{\mathrm{H}}\boldsymbol{H}$ is non-singular for any non-zero $\boldsymbol{h}_e$, then the diagonal elements of $[\boldsymbol{H}^{\mathrm{H}}\boldsymbol{H}]^{-1}$ satisfy the following inequality

$$[(\boldsymbol{H}^{\mathrm{H}}\boldsymbol{H})^{-1}]_{ll}^{-1} \geq c_0\|\boldsymbol{h}_e\|_F^2$$

for $l = 1, 2,\ldots,N$, where c_0 is a constant independent of $\boldsymbol{h}_e$.

Property 2: ([19]) For any non-zero vector $\boldsymbol{x}$, there exists $0 < C_{T\min} \leq C_{T\max} \leq 1$, and the matrix $(\mathcal{T}^{(K)}[\boldsymbol{x}])^{\mathrm{H}}\mathcal{T}^{(K)}[\boldsymbol{x}]$ satisfies the following inequality

$$C_{T\min}\|\boldsymbol{x}\|_F^{2K} \leq \det\left[\left(\mathcal{T}^{(K)}[\boldsymbol{x}]\right)^{\mathrm{H}}\mathcal{T}^{(K)}[\boldsymbol{x}]\right] \leq C_{T\max}\|\boldsymbol{x}\|_F^{2K}$$

From (4), the ZF detection for $\boldsymbol{s}_2$ is given by

$$\hat{\boldsymbol{s}}_2 = [\boldsymbol{H}]^{\dagger}\boldsymbol{y}_{T_1} = \alpha\sqrt{P_{\mathrm{T}}}\boldsymbol{s}_2 + [\boldsymbol{H}]^{\dagger}\boldsymbol{w}_{T_1} \tag{19}$$

Then, the noise covariance is

$$\begin{aligned}\boldsymbol{\Pi} &= \boldsymbol{R}^{-1}\\ &+ \alpha^2[\boldsymbol{H}]^{\dagger}\left(\sum_{m=1}^{M}\mathcal{T}^{N_1}\left[\boldsymbol{h}_{\Delta_2,m}\otimes\boldsymbol{t}_m\right]\left(\mathcal{T}^{N_1}\left[\boldsymbol{h}_{\Delta_2,m}\otimes\boldsymbol{t}_m\right]\right)^{\mathrm{H}}\right)\\ &([\boldsymbol{H}]^{\dagger})^{\mathrm{H}}\end{aligned}$$

where

$$\boldsymbol{R}^{-1} = [\boldsymbol{H}]^{\dagger}([\boldsymbol{H}]^{\dagger})^{\mathrm{H}} = (\boldsymbol{H}^{\mathrm{H}}\boldsymbol{H})^{-1}$$

Denote $\boldsymbol{\omega}_l$ as the lth column of $([\boldsymbol{H}]^{\dagger})^{\mathrm{H}}$, then the lth diagonal entry of the noise covariance is given by

$$\begin{aligned}\boldsymbol{\Pi}_{ll} &= \sigma_n^2\boldsymbol{\omega}_l^{\mathrm{H}}\boldsymbol{\omega}_l + \alpha^2\sigma_n^2\sum_{m=1}^{M}\boldsymbol{\omega}_l^{\mathrm{H}}\mathcal{T}^{N_1}\left[h_{\Delta_2,m}\otimes\boldsymbol{t}_m\right]\\ &\times\left(\mathcal{T}^{N_1}\left[\boldsymbol{h}_{\Delta_2,m}\otimes\boldsymbol{t}_m\right]\right)^{\mathrm{H}}\boldsymbol{\omega}_l\end{aligned}$$

Since $\mathcal{T}^{N_1}[\boldsymbol{h}_{\Delta_2,m}\otimes\boldsymbol{t}_m] = \mathcal{T}^{(N_1+Q-1)}[\boldsymbol{h}_{\Delta,m}]\mathcal{T}^{(N_1)}[\boldsymbol{t}_m]$ and

$$\begin{aligned}&\boldsymbol{\omega}_l^{\mathrm{H}}\mathcal{T}^{N_1}[\boldsymbol{h}_{\Delta,m}\otimes\boldsymbol{t}_m](\mathcal{T}^{N_1}[h_{\Delta,m}\otimes\boldsymbol{t}_m])^{\mathrm{H}}\boldsymbol{\omega}_l\\ &= \boldsymbol{\omega}_l^{\mathrm{H}}\mathcal{T}^{N_1+Q-1}[\boldsymbol{h}_{\Delta_2,m}]\mathcal{T}^{N_1}[\boldsymbol{t}_m](\mathcal{T}^{N_1}[\boldsymbol{t}_m])^{\mathrm{H}}\\ &\quad\left(\mathcal{T}^{N_1+Q-1}[\boldsymbol{h}_{\Delta_2,m}]\right)^{\mathrm{H}}\boldsymbol{\omega}_l\\ &< N_1\boldsymbol{\omega}_l^{\mathrm{H}}\mathcal{T}^{N_1+Q-1}[\boldsymbol{h}_{\Delta_2,m}]\left(\mathcal{T}^{N_1+Q-1}[\boldsymbol{h}_{\Delta_2,m}]\right)^{H}\boldsymbol{\omega}_l\\ &< N_1(N_1+Q-1)\|\boldsymbol{h}_{\Delta_2,m}\|_F^2\boldsymbol{\omega}_l^{\mathrm{H}}\boldsymbol{\omega}_l\end{aligned}$$

we obtain

$$\boldsymbol{\Pi}_{ll} < \sigma_n^2\left(1 + \gamma\sum_{m=1}^{M}\|\boldsymbol{h}_m\|_F^2\right)\boldsymbol{R}_{ll}^{-1} \tag{20}$$

where $\gamma = \alpha^2 N_1(N_1 + Q - 1)$. The symbol error probability under any given channel realisation $\boldsymbol{h}_e$ is expressed as [19]

$$P(\boldsymbol{h}_e, s_{2,l}) < \xi \exp\left(-\frac{a_i \alpha^2 P_T}{\sigma_n^2\left(1 + \gamma \sum_{m=1}^{M} \|\boldsymbol{h}_m\|_F^2\right)\boldsymbol{R}_{ll}^{-1}}\right) \quad (21)$$

where $\xi = (\mu - 1/\mu)$, $a_1 = (3/4(\mu - 1))$, $a_2 = (3/(2(\mu^2 - 1)))$ and $a_3 = ((\sin^2(\pi/\mu))/2)$ are constants for QAM, PAM and PSK constellations, respectively, with μ denoting the cardinality of the constellation.

Since $\boldsymbol{H}$ has full column rank for any non-zero $\boldsymbol{h}_e$, from the above Property 1, we have $(\boldsymbol{R}_{ll}^{-1})^{-1} \geq c_0\|\boldsymbol{h}_e\|_F^2$. Moreover, there is $\|\boldsymbol{h}_e\|_F^2 = \|\Theta_\Delta \boldsymbol{v}\|_F^2 \geq c_1\|\boldsymbol{v}\|_F^2$, where $c_1 = \lambda_{\min}(\Theta_\Delta^{\mathrm{H}}\Theta_\Delta)$. Under the condition that $\boldsymbol{\Theta}_\Delta$ has full column rank, that is, $c_1 > 0$, we directly arrive at $\left(\boldsymbol{R}_{ll}^{-1}\right)^{-1} \geq c\|\boldsymbol{v}\|_F^2$, where $c = c_0 c_1 > 0$.

As a result, we rewrite (21) as

$$P(\boldsymbol{h}_e, s_{2,l}) < \xi \exp\left(-\frac{a_i \alpha^2 c P_{\mathrm{T}}\|\boldsymbol{v}\|_F^2}{\sigma_n^2\left(1 + \gamma \sum_{m=1}^{M} \|\boldsymbol{h}_m\|_F^2\right)}\right) \quad (22)$$

Following the approximation that $\sum_{m=1}^{M} \|\boldsymbol{h}_m\|_F^2 = M$ when $M \gg 1$ [20, 21], we have

$$P(s_{2,l}) = E_{\boldsymbol{h}_e}\left\{P(\boldsymbol{h}_e, s_{2,l})\right\} < \xi \cdot E_{\boldsymbol{h}_e}\left\{\exp\left(-\sigma P_T\|\boldsymbol{v}\|_F^2\right)\right\} \quad (23)$$

where

$$\sigma = \frac{a_i \alpha^2 c}{\sigma_n^2(1 + \gamma M)}$$

Without loss of generality, we first assume $L_h \geq L_g$ in the following. Note that $\boldsymbol{v}_m = \mathcal{T}^{L_g}[\boldsymbol{h}_m]\boldsymbol{g}_m$, then $\boldsymbol{v} = \boldsymbol{\Gamma}\boldsymbol{g}$, where

$$\begin{aligned} \Gamma &= \mathrm{diag}\left(\mathcal{T}^{L_g}[\boldsymbol{h}_1], \quad \mathcal{T}^{L_g}[\boldsymbol{h}_2], \ \ldots, \mathcal{T}^{L_g}[\boldsymbol{h}_M]\right) \\ \boldsymbol{g} &= \left[\boldsymbol{g}_1^{\mathrm{T}}, \boldsymbol{g}_2^{\mathrm{T}}, \ \ldots, \boldsymbol{g}_M^{\mathrm{T}}\right]^{\mathrm{T}} \end{aligned} \quad (24)$$

Moreover, we know

$$\begin{aligned} P(s_{2,l}) &< \xi \cdot E_{\boldsymbol{h}_e}\left\{\exp\left(-\sigma P_T \boldsymbol{g}^{\mathrm{H}}\boldsymbol{\Gamma}^{\mathrm{H}}\boldsymbol{\Gamma}\boldsymbol{g}\right)\right\} \\ &= \xi \cdot E_{\boldsymbol{h}_m}\left\{\det\left[\boldsymbol{I} + \sigma P_T \boldsymbol{\Gamma}^{\mathrm{H}}\boldsymbol{\Gamma}\right]^{-1}\right\} \\ &= \xi \cdot \prod_{m=1}^{M} E_{\boldsymbol{h}_m}\left\{\det\left[\boldsymbol{I} + \sigma P_T\left(\mathcal{T}^{L_g}[\boldsymbol{h}_m]\right)^{\mathrm{H}}\mathcal{T}^{L_g}[\boldsymbol{h}_m]\right]^{-1}\right\} \\ &< \xi \cdot \prod_{m=1}^{M} E_{\boldsymbol{h}_m}\left\{\frac{1}{1 + \sigma^{L_g}P_T^{L_g}\det\left[\left(\mathcal{T}^{L_g}[\boldsymbol{h}_m]\right)^{\mathrm{H}}\mathcal{T}^{L_g}[\boldsymbol{h}_m]\right]}\right\} \end{aligned} \quad (25)$$

From the above Property 2, we obtain

$$\det\left[\left(\mathcal{T}^{L_g}[\boldsymbol{h}_m]\right)^{\mathrm{H}}\mathcal{T}^{L_g}[\boldsymbol{h}_m]\right] \geq c_3\|\boldsymbol{h}_m\|_F^{2L_g} \quad (26)$$

where $c_3 > 0$ is a constant. Then we arrive at

$$P(s_{2,l}) < \xi \cdot \prod_{m=1}^{M} E_{\boldsymbol{h}_m}\left\{\frac{1}{1 + \delta P_T^{L_g}\|\boldsymbol{h}_m\|_F^{2L_g}}\right\} \quad (27)$$

where $\delta = c_3\sigma^{L_g}$. Denote $\chi = \|\boldsymbol{h}_m\|_F^2$ for short and its probability density function is given by

$$f_\chi(x) = \frac{L_h(L_h x)^{L_h - 1}\mathrm{e}^{-L_h x}}{(L_h - 1)!} \quad (28)$$

Then, we have

$$\begin{aligned} E_{\boldsymbol{h}_m}\left\{\frac{1}{1 + \delta P_{\mathrm{T}}^{L_g}\|\boldsymbol{h}_m\|_F^{2L_g}}\right\} &= \int_0^\infty \frac{f_\chi(x)}{1 + \delta P_{\mathrm{T}}^{L_g}x^{L_g}}\mathrm{d}x \\ &= \frac{1}{(L_h - 1)!}\int_0^\infty \frac{x^{L_h - 1}\mathrm{e}^{-x}}{1 + \delta(P_{\mathrm{T}}/L_h)^{L_g}x^{L_g}}\mathrm{d}x \end{aligned} \quad (29)$$

1. When $L_g = L_h$, there is

$$\begin{aligned} &\int_0^\infty \frac{x^{L_g - 1}\mathrm{e}^{-x}}{1 + \delta(P_{\mathrm{T}}/L_h)^{L_g}x^{L_g}}\mathrm{d}x < \int_0^1 \frac{x^{L_g - 1}}{1 + \delta(P_{\mathrm{T}}/L_h)^{L_g}x^{L_g}}\mathrm{d}x \\ &\quad + \int_1^\infty \frac{\mathrm{e}^{-x}}{\delta(P_{\mathrm{T}}/L_h)^{L_g}}\mathrm{d}x \\ &= \left(\frac{\log\left(1 + \delta(P_{\mathrm{T}}/L_h)^{L_g}\right) + L_g\mathrm{e}^{-1}}{L_g\delta}\right)\frac{L_h^{L_g}}{P_{\mathrm{T}}^{L_g}} \end{aligned} \quad (30)$$

2. When $L_g < L_h$, there is

$$\begin{aligned} &\int_0^\infty \frac{x^{L_h - 1}\mathrm{e}^{-x}}{1 + \delta(P_{\mathrm{T}}/L_h)^{L_g}x^{L_g}}\mathrm{d}x < \int_0^1 \frac{x^{L_h - L_g - 1}}{\delta(P_{\mathrm{T}}/L_h)^{L_g}}\mathrm{d}x \\ &\quad + \int_1^\infty \frac{x^{L_h - L_g - 1}\mathrm{e}^{-x}}{\delta(P_{\mathrm{T}}/L_h)^{L_g}}\mathrm{d}x \\ &= \left(\frac{1}{L_h - L_g} + \mathrm{e}^{-1}\sum_{k=0}^{L_h - L_g - 1}\frac{(L_h - L_g - 1)!}{k!}\right)\frac{L_h^{L_g}}{\delta P_{\mathrm{T}}^{L_g}} \end{aligned} \quad (31)$$

Finally, combining (29)–(31), we can obtain a compact form as $P_T \to \infty$

$$E_{\boldsymbol{h}_m}\left\{\frac{1}{1 + \delta P_{\mathrm{T}}^{L_g}\|h_m\|_F^{2L_g}}\right\} < G_c \cdot \frac{1}{P_{\mathrm{T}}^{L_g}} \quad (32)$$

and

$$P(s_{2,l}) < \xi \cdot G_c^M \cdot P_{\mathrm{T}}^{-ML_g} \quad (33)$$

which indicates that a diversity of order ML_g is obtained, including both the cooperative and multipath diversity.

Bearing in mind that from (24) to (33), we consider only $L_h \geq L_g$. Note that $\boldsymbol{h}_m$ and $\boldsymbol{g}_m$ are symmetrical in (23). Thus, following (24)–(33), we can directly find out that a diversity of order ML_h is obtained when $L_h < L_g$. Hence, finally, the obtained diversity by the ZF receiver can be expressed as $M \cdot \min\{L_h, L_g\}$. Based on the fact that the linear MMSE receiver is superior to or, at least, equivalent to the ZF receiver, this lemma is proved.

IET Commun., 2013, Vol. 7, Iss. 2, pp. 137–145
doi: 10.1049/iet-com.2012.0440

11 Appendix 3

11.1 Proof of Lemma 2

We define the Q-length Vandermonde vectors $\boldsymbol{a}_m = \left[1, a_m, \ldots, a_m^{Q-1}\right]^{\mathrm{T}}$, and

$$\tilde{\underline{\boldsymbol{t}}}_{\Delta,m} = \left[\boldsymbol{0}_{1\times\left(\tau_{2,m}^{(1)}+\tau_{1,m}^{(2)}\right)}, \ \boldsymbol{t}_m^{\mathrm{T}}\mathrm{diag}(\boldsymbol{a}_m), \ \boldsymbol{0}_{1\times\left(L_{\max}^{(1)}-\tau_{2,m}^{(1)}+\tau_{1,\max}^{(2)}-\tau_{1,m}^{(2)}\right)}\right]^{\mathrm{T}}$$

$$\tilde{\underline{\boldsymbol{\Theta}}}_{\Delta} = \left[\mathcal{T}^{(L)}[\tilde{\underline{\boldsymbol{t}}}_{\Delta,1}], \quad \mathcal{T}^{(L)}[\tilde{\underline{\boldsymbol{t}}}_{\Delta,2}], \quad \ldots, \quad \mathcal{T}^{(L)}[\tilde{\underline{\boldsymbol{t}}}_{\Delta,M}]\right]$$

Define

$$G(a_1, a_2, \ldots, a_M) = \det\left[\tilde{\underline{\boldsymbol{\Theta}}}_{\boldsymbol{\Delta}}^{\mathrm{H}}\tilde{\underline{\boldsymbol{\Theta}}}_{\boldsymbol{\Delta}}\right] \tag{34}$$

which is a polynomial in several variables and hence is analytical. To establish the desired result, it suffices to show that $G(a_1, a_2,\ldots,a_M)$ is non-trivial. Let $a_m = a$, that is, a_m becomes identical. The key observation here is that at this situation, $\tilde{\underline{\boldsymbol{\Theta}}}_{\boldsymbol{\Delta}}$ has the same rank property with $\boldsymbol{\Theta}_{\boldsymbol{\Delta}}$. Thus, when $\boldsymbol{t}_m$ is carefully designed such that $\boldsymbol{\Theta}_{\boldsymbol{\Delta}}$ has full column rank under any delay profile, we have $G(a, a,\ldots, a) \neq 0$. This shows that $G(a_1, a_2,\ldots,a_M)$ is a non-trivial polynomial. According to the analytical function Lemma 2 in [22], $G(a_1, a_2,\ldots,a_M)$ is non-zero almost everywhere, except for a measure zero subset, which implies that $\tilde{\underline{\boldsymbol{\Theta}}}_{\boldsymbol{\Delta}}$ has full column rank almost surely (in the measured theoretical sense).